Journal of Superconductivity: Incorporating Novel Magnetism, Vol. 16, No. 2, April 2003 (© 2003)

Theory of Cyclotron Resonance and Magneto-Optics in n- and p-Type InMnAs in Ultra-high Magnetic Fields

G. D. Sanders,[1] Y. Sun,[1] C. J. Stanton,[1] G. A. Khodaparast,[2] J. Kono,[2] Y. H. Matsuda,[3,4] N. Miura,[3] T. Słupinski,[5,6] A. Oiwa,[5] and H. Munekata[5]

Received September 30, 2002

We present a theory for the electronic and optical properties of n- and p-type $In_{1-x}Mn_xAs$ in ultra-high magnetic fields. An eight-band effective mass model based on the Pidgeon–Brown model and including the wavevector dependence of the electronic states as well as the *s–d* and *p–d* exchange interactions with Mn d-electrons is used to determine the electronic states. The optical properties such as cyclotron resonance are computed using Fermi's golden rule. Comparison of the theory with ultra-high magnetic field (>50 T) cyclotron resonance experiments shows that the electron cyclotron resonance peak shifts with Mn doping and that the shift allows one to extract the Mn-electron/hole exchange parameters, α and β. The hole cyclotron resonance shows multiple resonance peaks, which we attribute a heavy to heavy and light to light hole transitions.

KEY WORDS: cyclotron resonance; dilute magnetic semiconductors; ultra-high magnetic fields.

1. INTRODUCTION

Dilute magnetic semiconductor alloys of narrow-gap $In_{1-x}Mn_xAs$ have recently attracted much attention both experimentally and theoretically. Narrow-gap materials involve conduction and valence band mixing, and Mn doping gives rise to enhanced *g*-factors for both electrons and holes. Ferromagnetism in these alloys has also been observed. The electronic and optical properties of $In_{1-x}Mn_xAs$ is important for designing ferromagnetic heterostructures and spintronic devices with high Curie temperatures.

In this paper, we present theoretical results for ultra-high (>50 T) magnetic field cyclotron resonance (CR) in n- and p-doped InMnAs and compare them to experiment. Our results show a shift in the electron cyclotron resonance with Mn doping, which is sensitive to the Mn-electron/hole sp–d exchange interaction and allows one to determine the exchange parameters α and β. For the hole cyclotron resonance, we are able to identify the several peaks seen in the experiments and associate them with a heavy hole to heavy hole and a light hole to light hole transition.

2. EFFECTIVE MASS THEORY

We have developed a theory for electronic and magneto-optical properties in n- and p-type narrow-gap $In_{1-x}Mn_xAs$ dilute magnetic semiconductor (DMS) alloys in an ultra-high magnetic field, B, oriented along [001]. Our theory builds on the eight-band effective mass Pidgeon–Brown model [1], which we have generalized to include (i) the energies and electronic states as a function of the wavevector parallel to B, and (ii) s–d and p–d exchange interactions

[1]Department of Physics, University of Florida, Gainesville, Florida 32611-8440.
[2]Department of Electrical and Computer Engineering, Rice Quantum Institute and Center for Nanoscale Science and Technology, Rice University, Houston, Texas 77005.
[3]Institute for Solid State Physics, University of Tokyo, Kashiwa, Chiba 277-8581, Japan.
[4]Present address: Department of Physics, Okayama University, Okayama, Japan.
[5]Imaging Science and Engineering Laboratory, Tokyo Institute of Technology, Yokohama, Kanagawa 226-8503, Japan.
[6]Present address: Institute of Experimental Physics, Warsaw University, Hoza 69, 00-681 Warsaw, Poland.

0896-1107/03/0400-0449/0

with the localized *Mn* d-electrons. Our model couples electrons, heavy holes, light holes, and split-off holes. The exchange coupling of free carriers to the localized *Mn* d-electrons is parameterized by exchange integrals α and β defined in [2].

In calculating band structure, we assume we are in the paramagnetic phase and compute the magnetization using a simple Brillouin function expression [3]. We then compute the Fermi level as a function of temperature, magnetic field, *Mn* concentration, and free electron or hole concentration (n or p).

Magneto-optical properties are obtained using Fermi's golden rule to compute the absorption coefficient for arbitrary polarizations [4]. The magneto-optical absorption coefficient at the photon energy $\hbar\omega$ is [4]

$$\alpha(\hbar\omega) = \frac{\hbar\omega}{(\hbar c)n_{\mathrm{r}}}\epsilon_2(\hbar\omega) \tag{1}$$

where $\epsilon_2(\hbar\omega)$ is the imaginary part of the dielectric function and n_{r} is the index of refraction. The imaginary part of the dielectric function is found using Fermi's golden rule. The result is

$$\epsilon_2(\hbar\omega) = \frac{e^2}{\lambda^2(\hbar\omega)^2}\sum_{n,\nu,n',\nu'}\int_{-\infty}^{\infty} dk_z|\hat{e}\cdot\vec{P}_{n,\nu}^{n',\nu'}(k_z)|^2 \times(f_{n,\nu}(k_z) - f_{n',\nu'}(k_z))\,\delta\left(\Delta E_{n,\nu}^{n',\nu'}(k_z) - \hbar\omega\right), \tag{2}$$

where $\left(\Delta E_{n,\nu}^{n',\nu'}(k_z) = E_{n',\nu'}(k_z) - E_{n',\nu'}(k_z)\right.$ is the transition energy and $\lambda = \sqrt{\hbar c/eB}$ is the magnetic length. The function $f_{n,\nu}(k_z)$ in Eq. (2) is the probability that the state (n, ν, k_z), with energy $E_{n,\nu}(k_z)$, is occupied (see Ref. 2 for a more detailed explanation of the notation). It is given by the Fermi distribution function and depends on the net carrier density. $\vec{P}_{n,\nu}^{n',\nu'}(k_z)$ is the optical matrix element between states (n, ν, k_z) and (n', ν', k_z), and $\hat{e}$ is the polarization of the light. In determining the optical matrix element, we use a standard set of $\mathbf{k}\cdot\mathbf{p}$ band parameters for InAs.[5].

Band filling effects are explicitly considered in computing the optical properties and depend critically on the carrier densities, which are deduced from Hall measurements [6]. The Dirac delta functions appearing in the Fermi's golden rule transition probability is replaced by a Lorentzian lineshape whose full width at half maximum (FWHM) is an input parameter.

3. N-TYPE RESULTS

3.1. Cyclotron Resonance (CR)

We have performed CR measurements on $In_{1-x}Mn_xAs$ films as described in [6] and compared the experimental results with our theory. Experimental and theoretical CR absorption spectra in the Faraday configuration at 30 K are shown in Fig. 1 as functions of the magnetic field for $x = 0$, 2.5, 5, and 12%. The radiation is e-active circularly polarized with photon energy $\hbar\omega = 0.117$ eV. In Fig. 1a), the experimentally measured CR absorption is proportional to the negative of the CR transmission and in Fig. 1b, the calculated CR absorption based on our theory is shown. In the calculation, the curves were broadened based on the experimentally measured mobilities [6]. All the samples show pronounced absorption peaks and the resonance field is seen to decrease with increasing x.

In a simple theory, all conduction band states with a given spin would shift by an amount proportional to $x\,\alpha\langle S_z\rangle$ where $\langle S_z\rangle$ is the average *Mn* spin along the field. Since all states of a given spin would shift by the same amount, the cyclotron resonance would not be sensitive to the *Mn* concentration. However, in narrow-gap systems, owing to conduction and valence band mixing, the shift depends on both α and β as well as x.

3.2. Exchange Integrals

In Fig. 2, we plot the electron cyclotron mass as a function of the *Mn* concentration for the lowest lying

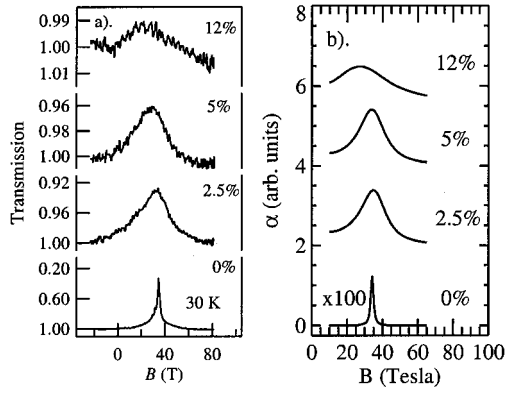

Fig. 1. Cyclotron resonance absorption in n-type $In_{1-x}Mn_xAs$ at 30 K as function of B for $x = 0$, 2.5, 5, and 12%. (a) Experimental CR transmission (plotted with decrease along positive y) and (b) calculated CR absorption. Note CR peak shift with increasing x.

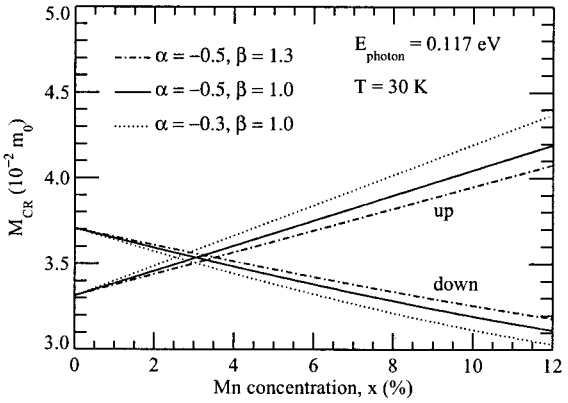

Fig. 2. Electron cyclotron mass at 30 K in *n*-type $In_{1-x}Mn_xAs$ for the lowest spin-up and spin-down Landau level transitions as a function of x for several combinations of the exchange integrals α and β (in units of eV).

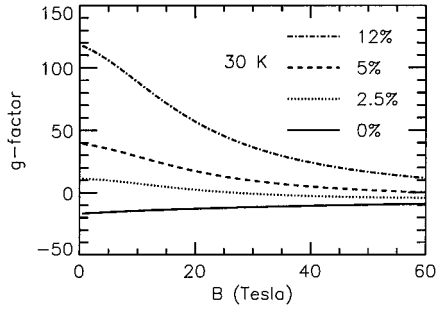

Fig. 3. Electron g-factors in n-type $In_{1-x}Mn_xAs$ at $T = 30$ K as a function of B for $x = 0, 2.5, 5$, and 12%.

spin-up and spin-down Landau level transitions. Note that changing either α and β effects the positions of the peaks. Results empirically indicate that the shift depends on the difference $\beta - \alpha$ to lowest order. We find that the values of α and β that best reproduce the experimental trends are $\alpha = 0.5$ eV and $\beta = -1.0$ eV. These values could change slightly depending upon the exact choice of the parameters used in the $\mathbf{k} \cdot \mathbf{p}$ calculation.

3.3. *g*-Factors

In the absence of Mn impurities, it is well known that at low magnetic fields, the spin splittings between the spin-up and spin-down Landau levels can be described in terms of an effective gyromagnetic factor [7]

$$g^* = 2\left(1 - \frac{E_p}{3E_g}\frac{\Delta}{E_g + \Delta}\right) \tag{3}$$

where E_g is the band gap, Δ is the spin–orbit splitting, and E_p is the optical matrix parameter. The g-factor in Eq. (3) depends on temperature through the temperature-dependent band gap. For bulk InAs at $T = 30$ K we find $g^* = -14.7$. At nonzero B fields, the above expression for the gyromagnetic factor in Eq. (3) is not correct. As a function of B, the spin splittings become nonlinear and in addition depend explicitly on the Landau subband level and wavevector $\mathbf{k}$.

In Fig. 3 the calculated lowest electron Landau level gyromagnetic factor for the zone center is plotted as a function of B for four different values of x. In all cases, doping with *Mn* impurities is seen to increase the g-factor (it changes sign with high doping) and the effect is seen to be sensitive to both the temperature and the *Mn* concentration.

4. P-TYPE RESULTS

We have also performed hole cyclotron resonance experiments on p-doped InMnAs samples and compared with our theory. In the upper panel of Fig. 4 experimental and theoretical CR curves are plotted as a function of the applied magnetic field in p-doped InAs.

The experimental curve is the negative of the transmission and is offset for clarity and plotted in arbitrary units. The theoretical curve is plotted in units of cm^{-1}. The radiation is h-active circularly polarized with photon energy $\hbar\omega = 0.117$ eV. In the theoretical CR curve, lines are *not* broadened and the FWHM linewidth is taken to be $\gamma = 4$ meV for the numerical calculations. The carrier density in the calculation is $p = 10^{19}$ cm^{-3} so that for $T = 30$ K and $B > 30$ T, the Fermi energy is such that the first two Landau subbands are occupied. For lower carrier densities, only one strong transition is seen in the calculation. These results indicate that itinerant carries are present in these experiments.

Holes optically excited from these two subbands give rise to the two strong cyclotron absorption peaks labeled 1 and 2. Only the zone center Landau subband energies involved in these two cyclotron resonance transitions are shown in the lower panel of Fig. 4. The cyclotron absorption peak, 2, near 40 T is due to transitions between the spin-down ground-state heavy hole Landau subband, $H_{-1,1}$, with energy $E_{-1,1}(k_z)$ and the Landau subband, $H_{0,2}$, with energy $E_{0,2}(k_z)$. Near the zone center $H_{0,2}$ is primarily spin-down heavy hole in character which accounts for our use of the "H" designation for this subband. The cyclotron absorption

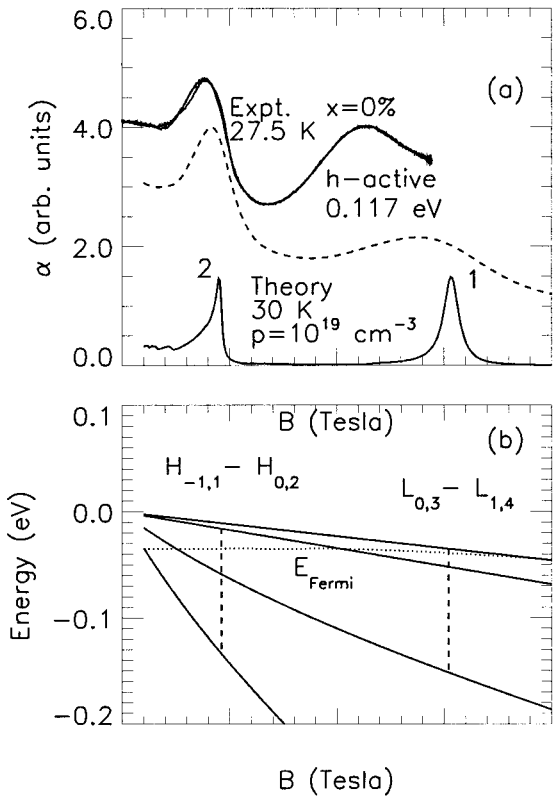

Fig. 4. (a) Experimental and theoretical cyclotron absorption as a function of B in p-type *InAs* for h-active circularly polarized light with $\hbar\omega = 0.117$ eV. The solid theory curve is broadened with a minimal 4 MeV linewidth while the dashed theory curve is broadened with a 40 MeV linewidth. (b) $k = 0$ energies of the Landau subbands responsible for peaks 1 and 2.

peak, 1, seen around 140 T is a spin-down light hole transition between the $L_{0,3}$ and $L_{1,4}$ subbands. The CR peaks 1 and 2 are seen to be asymmetric about their respective resonance fields.

For $B < 30$ T, higher Landau subbands become occupied and excitation of holes from these subbands is responsible for the downward sloping plateau seen in the CR absorption for $B < 30$ T. Results for p-doped InMnAs will be discussed later [8].

5. CONCLUSIONS

In summary, we have calculated ultra-high magnetic field CR in $In_xMn_{1-x}As$ and studied its dependence on the Mn doping concentration x. The electron cyclotron resonance peak shifts with x and through comparison with experiment, allows one to extract the sp–d electron/hole-*Mn* ion exchange interactions α and β. The electron g-factor at high doping and low magnetic fields can be quite large (>100). For p-doped samples, the calculated hole CR shows multiple peaks, which agrees with experiments. These results show that there are itinerant carriers in this system.

ACKNOWLEDGMENTS

This work was supported by DARPA through grant No. MDA 972-00-1-0034 and the NEDO International Joint Research Program.

REFERENCES

1. C. K. Pidgeon and R. N. Brown, *Phys. Rev.* **146,** 575 (1966).
2. J. Kossut, *Semicond Semimetals* **25,** 183 (1988).
3. J. K. Furdyna, *J. Appl. Phys.* **64,** R29 (1988).
4. F. Bassani and G. P. Parravicini, *Electronic States and Optical Transitions in Solids* (Pergamon, New York, 1975).
5. I. Vurgaftman, J. R. Meyer, and L. R. Ram-Mohan, *J. Appl. Phys.* **89,** 5815 (2001).
6. M. A. Zudov, J. Kono, Y. H. Matsuda, T. Ikaida, N. Miura, H. Munekata, G. D. Sanders, and C. J. Stanton, *Phys. Rev. B* **66,** 161307(R), (2002).
7. C. Rigaux, *Semicond Semimetals* **25,** 229 (1988).
8. G. A. Khodaparast, M. A. Zudov, J. Kono, Y. H. Matsuda, T. Ikaida, S. Ikeda, N. Miura, T. Slupinski, A. Oiwa, H. Munekata, G. D. Sanders, Y. Sun, and C. J. Stanton, *J. Supercond.* **16**(1), 107 (2003).